Solid Earth, 5, 409–424, 2014
www.solid-earth.net/5/409/2014/
doi:10.5194/se-5-409-2014

Solid Earth Open Access

BrO / SO_2 molar ratios from scanning DOAS measurements in the NOVAC network

P. Lübcke[1,2], N. Bobrowski[1], S. Arellano[3], B. Galle[3], G. Garzón[4], L. Vogel[1,*], and U. Platt[1]

[1]Institute of Environmental Physics, University of Heidelberg, Heidelberg, Germany
[2]Max Planck Institute for Chemistry, Mainz, Germany
[3]Department of Earth and Space Sciences, Chalmers University of Technology, Gothenburg, Sweden
[4]FISQUIM Research Group, Laboratory Division, Colombian Geological Survey, Cali, Colombia
[*]now at: Earth Observation Science Group, Space Research Centre, Department of Physics and Astronomy, University of Leicester, Leicester, UK

Correspondence to: P. Lübcke (pluebcke@iup.uni-heidelberg.de)

Received: 30 September 2013 – Published in Solid Earth Discuss.: 5 November 2013
Revised: 25 March 2014 – Accepted: 31 March 2014 – Published: 4 June 2014

Abstract. The molar ratio of BrO to SO_2 is, like other halogen / sulfur ratios, a possible precursor for dynamic changes in the shallow part of a volcanic system. While the predictive significance of the BrO / SO_2 ratio has not been well constrained yet, it has the major advantage that this ratio can be readily measured using the remote-sensing technique differential optical absorption spectroscopy (DOAS) in the UV. While BrO / SO_2 ratios have been measured during several short-term field campaigns, this article presents an algorithm that can be used to obtain long-term time series of BrO / SO_2 ratios from the scanning DOAS instruments of the Network for Observation of Volcanic and Atmospheric Change (NOVAC) or comparable networks. Parameters of the DOAS retrieval of both trace gases are given. The influence of co-adding spectra on the retrieval error and influences of radiative transfer will be investigated. Difficulties in the evaluation of spectroscopic data from monitoring instruments in volcanic environments and possible solutions are discussed. The new algorithm is demonstrated by evaluating data from the NOVAC scanning DOAS systems at Nevado del Ruiz, Colombia, encompassing almost 4 years of measurements between November 2009 and end of June 2013. This data set shows variations of the BrO / SO_2 ratio several weeks prior to the eruption on 30 June 2012.

1 Introduction

The molar ratio of halogen (mainly HCl, HF) to sulfur species (mainly SO_2) in volcanic plumes has long been known as a possible tracer for volcanic activity (e.g. Noguchi and Kamiya, 1963; Menyailov, 1975; Pennisi and Le Cloarec, 1998). This is due to the different solubility of volatiles in magma (e.g. Carroll and Holloway, 1994) and its dependence on pressure. As a consequence, different gaseous species are exsolved in equilibrium at different magmastatic pressures, i.e. at different depths in the magma column. The most commonly used example of halogen / sulfur ratios has been the measurement of the HCl/SO_2 molar ratio (e.g. Noguchi and Kamiya, 1963). Another halogen species is BrO, which has now been detected at several volcanoes (e.g. Bobrowski et al., 2003; Bobrowski and Platt, 2007; Boichu et al., 2011; Kelly et al., 2012; Hörmann, 2013) and whose abundance was suggested as an additional indicator for changes in volcanic activity (Bobrowski and Giuffrida, 2012). One major advantage of measuring the BrO / SO_2 molar ratio is that both species can be detected in a single spectroscopic remote sensing measurement using differential optical absorption spectroscopy (DOAS) in the UV (Platt and Stutz, 2008), which is a rather simple-to-implement and sensitive technique.

Scanning DOAS has become the most widespread method for measuring the emission rate of volcanic SO_2 (e.g. Galle et al., 2003). In particular, within the framework of the EU project NOVAC (Network for Observation of Volcanic and

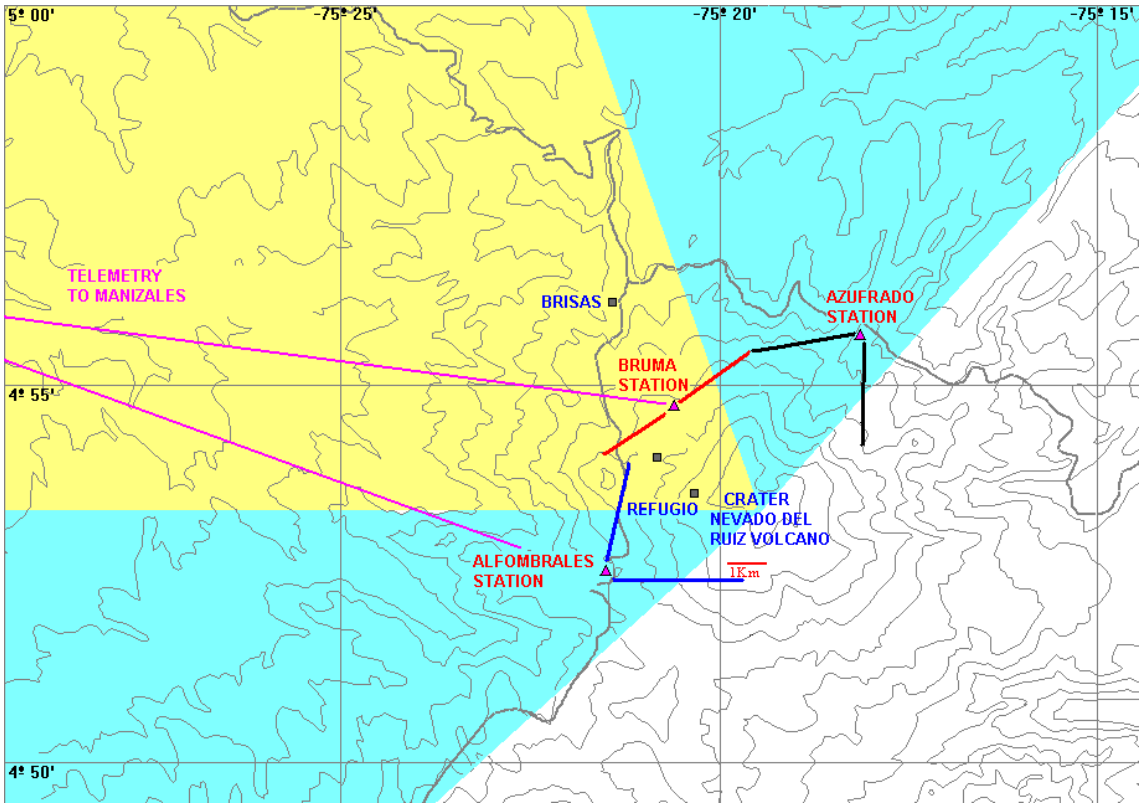

Figure 1. Topographic map (contour levels every 200 m, the upper contour level is at 5200 m, Bruma station is at 4800 m a.s.l.) showing the location of Nevado del Ruiz volcano (Colombia) and the three NOVAC stations used for gas monitoring. The blue, red and black lines depict the viewing directions of the scanning DOAS systems. The two original instruments at Alfombrales Station and Bruma Station were installed in November 2009 and transmit data in real time to the volcanological observatory located at Manizales city. The third instrument at Azufrado Station was installed in May 2012; its data are not included in this paper. The yellow background colour shows the wind direction for approximately 70 % of the time, and the light blue shaded area shows the wind direction for the remaining 30 %.

Atmospheric Change, Galle et al., 2010) to date about 70 scanning DOAS systems have been installed at 26 volcanoes worldwide, with the goal of performing automated spectroscopic gas emission rate measurements. These instruments measure the volcanic SO_2 emission rates by acquiring scattered UV radiation spectra over a scan through a surface intercepting the volcanic plume and combining the DOAS-derived gas column densities with geometrical factors and the component of transport speed normal to the scanned surface. Typically, about 40 individual gas emission rate measurements are obtained daily at each volcano by NOVAC instruments, which have allowed operational volcanic gas monitoring to approach temporal resolutions comparable to other methods of geophysical surveillance.

While the spectra are routinely evaluated for SO_2 by the local observatories, this is not the case for BrO. The BrO absorption cross section (in this work the one of Fleischmann et al., 2004, is used) is roughly a factor of 150 larger than that of SO_2 (in this work the one of Vandaele et al., 2009, is used) in the wavelength ranges typically used for DOAS evaluations (Vogel, 2011), but the abundance of BrO is significantly lower. BrO / SO_2 ratios between 8×10^{-5} and 1×10^{-3} have been found in volcanic plumes (Bobrowski and Platt, 2007), thus leading to one to two orders of magnitude weaker BrO absorption structures compared to SO_2. The smaller optical density makes it technically more challenging to detect and accurately measure BrO. In particular, small instrumental imperfections like changes in the instrument's slit function and the wavelength-channel alignment due to, for example, changes of the instrument's temperature (e.g. Chapter 3 in Kern, 2009), which have only a negligible effect on the SO_2 evaluation, pose a challenge for the BrO evaluation. Additionally, the noise due to photon statistics has to be lower in order to obtain a good signal to noise ratio for the BrO evaluation. One way to achieve this is by co-adding several spectra obtained by the same instrument under similar measurement conditions (e.g. within the same horizon-to-horizon scan or from consecutive scans with close time proximity).

This work presents an algorithm to evaluate the spectra recorded by the NOVAC instruments in order to obtain BrO column densities and BrO / SO_2 ratios. We give detailed

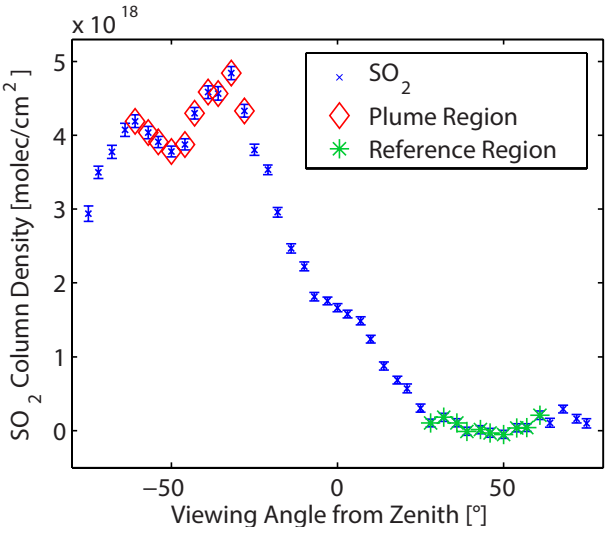

Figure 2. Example of the SO_2 column densities from one complete scan ($-75°$ – zenith – $+75°$ elevation angle, measured clockwise when looking towards the volcano). The red diamonds show the column densities defining the volcanic plume region, while the green asterisks show the column densities defining the reference region.

information about the parameters of the DOAS evaluation used for the analysis of the NOVAC spectra. The feasibility of the BrO evaluation will be demonstrated as well as the magnitude of DOAS fit errors. As an example, a first long-term time series from the Colombian volcano Nevado del Ruiz (see Fig. 1) is presented.

2 Method

2.1 Evaluation procedure

The NOVAC Version 1 instruments installed at all volcanoes in NOVAC use a "flat" or "conical" scanning geometry; that is, all viewing directions of a scan lie in a plane or on the surface of a semi-cone open towards the volcano (Galle et al., 2010). The set of consecutive scattered sunlight spectra collected from horizon to horizon (in this work only viewing directions between $-75°$ to $+75°$ elevation angle were evaluated) is referred to as a plume scan in the following. The instruments utilize Ocean Optics S2000 spectrometers (with a wavelength range of 280–425 nm and an optical resolution of ≈ 0.6 nm) that are not thermally stabilized, which results in a robust, energy-efficient design suitable for operation in remote locations that are sometimes difficult to access.

All spectra of each plume scan are pre-evaluated for SO_2 using a zenith spectrum acquired at the beginning of each plume scan as a reference spectrum. At this time underexposed and overexposed spectra (intensity below 15 % or above 85 % of the maximum exposure in the spectral region used for the DOAS evaluation) were removed from further evaluation. In the next step, the 10 adjacent spectra with the highest mean SO_2 column density (CD) value are selected and defined as the volcanic plume region. Then a set of 10 adjacent spectra with the lowest mean SO_2 value is defined as the reference region (see Fig. 2). Next, the spectra from the plume region are co-added to obtain a collective plume spectrum with higher signal to noise ratio, as well as the spectra from the reference region to obtain a collective reference spectrum.

The collective plume and reference spectra are then evaluated using the DOAS method (see below). To obtain an even better signal to noise ratio, we also co-added the collective reference and plume spectra of four consecutive scans and evaluated the resulting spectra, which improved our BrO detection limit by a factor of two. Depending on the time of day, four consecutive scans are typically recorded within 15–60 min. A flow chart of the data processing procedure is shown in Fig. 3.

2.2 Spectroscopic retrieval

All spectra are evaluated with a fitting routine that combines a non-linear Levenberg–Marquardt fit and a standard least-squares fit (Platt and Stutz, 2008) using the DOASIS software package (Kraus, 2006).

For all evaluations, the reference spectrum is first wavelength calibrated using a high-resolution solar spectrum (Chance and Kurucz, 2010) that was convoluted with the line shape of the 334.15 nm line of a low-pressure mercury lamp to match the lower spectral resolution of the spectrometers used in the NOVAC instruments (of about 0.6 nm FWHM – full width at half maximum). This line of the Hg spectrum was also used for the convolution of the high-resolution absorption cross sections; it was selected due to its proximity to the spectral region of interest for our evaluations. The calibration from the reference spectrum is also used for the plume spectra. The fit coefficient of the reference spectrum in the DOAS fit is fixed to -1. Two Ring spectra are included in the DOAS fit to correct for the Ring effect (Grainger and Ring, 1962). The first Ring spectrum is a standard Ring spectrum calculated using the DOASIS software package; the second is created from the first Ring spectrum by multiplying it with a wavelength-dependent term (in this work λ^{-4}) to account for multiple Rayleigh scattering in the atmosphere (Wagner et al., 2009).

A third-order polynomial is included in the fit to account for broadband absorption structures and Rayleigh as well as Mie scattering structures in the spectra. An additional wavelength-independent offset in the intensity space is allowed to correct for stray light inside the spectrometer.

The SO_2 evaluation is performed in the wavelength range between 314.8 nm and 326.8 nm including one SO_2 absorption cross section at 298 K (Vandaele et al., 2009) and one O_3 absorption cross section at 221 K (Burrows et al., 1999).

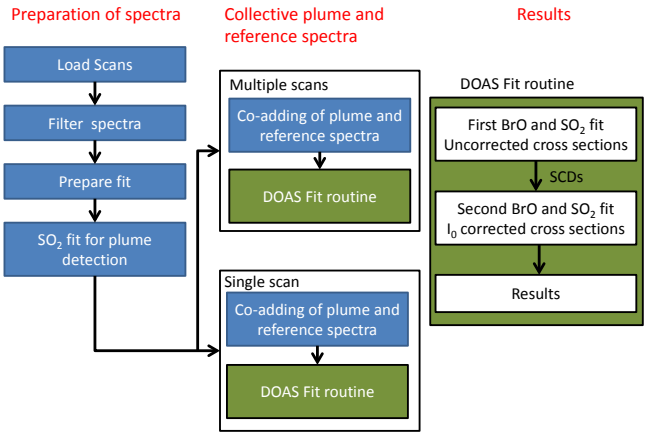

Figure 3. Flow chart of the data evaluation to automatically retrieve BrO/SO_2 ratios.

The BrO evaluation is performed between 330.6 nm and 352.75 nm using the following absorption cross sections: BrO at 298 K (Fleischmann et al., 2004), the same SO_2 and O_3 as above, O_4 (Hermans, 2003), NO_2 at 298 K (Vandaele et al., 1998) and CH_2O at 298 K (Meller and Moortgat, 2000). An example of a BrO fit is shown in Fig. 4. The evaluation ranges and trace gases included in the SO_2 as well as in the BrO fit were chosen according to Vogel (2011) and Vogel et al. (2013), who performed a series of studies on the optimal evaluation wavelength range for BrO and SO_2 in a combination of real measurement data and theoretical studies.

To verify the results, both trace gases were also evaluated in additional wavelength ranges. SO_2 was additionally evaluated between 326.5 and 353.3 nm, a wavelength range already used by Hörmann et al., 2013, as an additional wavelength range for the SO_2 retrieval. BrO was additionally evaluated between 327 and 347 nm. This wavelength range was used by Kelly et al., 2013, for the BrO retrieval.

All trace gas reference cross sections are convoluted to match the instrument resolution using the 334.15 nm line of a mercury lamp, a sample of the instrument line shape, recorded with the respective spectrometer. To account for the I_0 effect (Platt and Stutz, 2008), an iterative approach is used. First, a fit is performed to retrieve uncorrected column densities of the trace gases; these column densities are then used to create I_0-corrected absorption cross sections (Wagner et al., 2002).

In order to correct for small inaccuracies in the wavelength calibration, the reference spectrum and both Ring spectra, as one set, and all trace gas absorption cross sections, as another set, are allowed to be shifted and squeezed against the measurement spectrum. A shift of ± 0.2 nm and a squeeze of 0.98–1.02 were allowed.

2.3 Temperature influences on the DOAS retrieval

The instruments installed at Nevado del Ruiz are not thermally stabilized. While this greatly improved the robustness of these instruments, it should be noted that variations of the spectrometer's temperature can lead to problems in the DOAS retrieval.

Figure 5 shows the range of temperatures the instruments at Nevado del Ruiz are exposed to and that the temperature has an effect on the instrument calibration as well as the instrumental line shape. In general variations of the instrument's wavelength calibration are not a problem as spectra can be calibrated against a high-resolution solar spectrum, an approach also used here.

However, there are two problems if the instrument's optical alignment changes: the first problem appears when co-adding spectra. The spectral intensities are summed up for each channel; if the pixel-wavelength alignment changes between different spectra which are co-added, the resulting spectrum can be erroneous. However, the temperature changes slowly, and most spectra that are co-added were recorded within a time of 15 min up to 1 h. Therefore, this effect should be negligible.

The second effect of the instrument's temperature regards the instrumental line shape. Currently, all spectra are convolved with the 334.15 nm line of a mercury lamp that was recorded at room temperature. Instrumental characterization of S2000 spectrometers performed within the NOVAC project (i.e. Pinardi, 2007, or Kern, 2009) reported changes of up to 10 % for the SO_2 column densities caused by temperature-induced changes of the instrument line shape for temperatures between 5 and 40 °C (comparable to the temperatures occurring at Nevado de Ruiz).

To assess the error due to the second effect, we performed studies using synthetic spectra (similar to Vogel, 2011). A measurement spectrum containing a BrO CD of 1.5×10^{14} molecules cm^{-2} and an SO_2 CD of 1×10^{18} molecules cm^{-2} and a Fraunhofer reference spectrum free of volcanic absorbers were simulated (see Appendix for details). The measurement spectrum and Fraunhofer reference spectrum were convolved to match the lower resolution of a theoretical instrument with a Gaussian profile with varying FWHM (steps of 0.025 nm between 0.525 nm and 0.775 nm). The absorption cross sections for the DOAS retrieval of all spectra were convolved with a Gaussian profile with a FWHM of 0.65 nm. After preparation each set of spectra (measurement and Fraunhofer reference spectrum convolved with the same Gaussian profile) was evaluated using the DOAS retrieval described above. The results of these evaluations are shown in Fig. 6. The BrO/SO_2 ratio deviates up to 15 % if the instrument line shape varies up to ± 0.125 nm (which is a slightly larger range than can be typically observed for the NOVAC instruments).

Since for most NOVAC spectrometers there are no records of the particular instrument's line shape at different

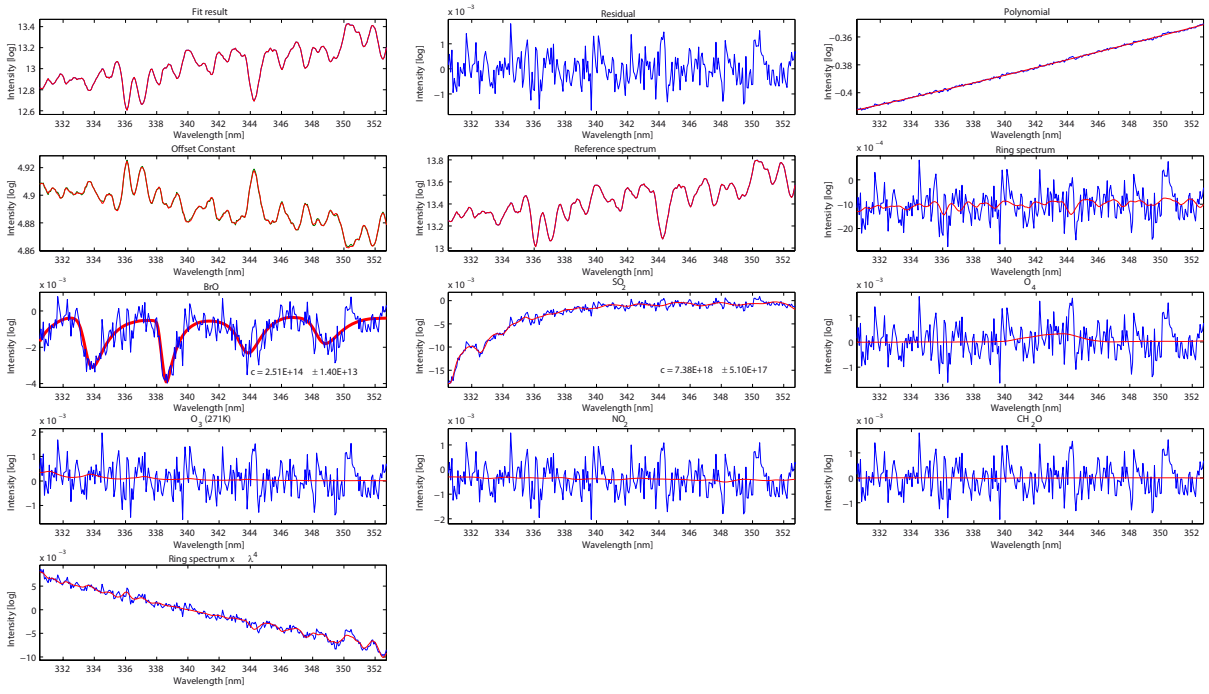

Figure 4. Example of a DOAS BrO evaluation performed in the wavelength range of 330.6–352.75 nm. The red lines show the fit, the blue lines the measurement data. A reference spectrum and two Ring spectra were included in the DOAS fit. The BrO column density is 2.51×10^{14} molecules cm^{-2}. Besides BrO, other trace gases (SO_2, O_4, O_3, NO_2, and CH_2O) were included in the DOAS evaluation. The spectra recorded for this example were recorded on 31 October 2012 between 16:32 and 17:05 GMT.

temperatures available, one possible way to further improve data quality would be to determine the instrument line shape from a comparison between the high-resolution solar reference spectrum and measurement spectra at different temperatures.

2.4 Radiative transfer modelling

The distance between the instrument and the volcanic plume and clouds can both influence the retrieved trace gas CDs. To assess the order of magnitude of errors due to these influences, we performed calculations using the 3-D radiative transfer model McArtim (Deutschmann, 2011). The SO_2 and BrO CDs were approximated by simulations at the centre of the wavelength interval used for the DOAS evaluation (320 nm for SO_2 and 340 nm for BrO).

A volcanic plume with a circular cross-section shape with diameter 1 km in the $x - z$ plane was simulated. The plume centred at 6 km altitude and was assumed to be infinitely extended in the y direction (see Fig. 7). Typical profiles of the trace gases O_3, O_4 and NO_2 and a Rayleigh atmosphere were used to account for non-volcanic absorbers and scattering. Trace-gas concentrations of SO_2 and BrO were set to 1×10^{13} molecules cm^{-3} and 1×10^{9} molecules cm^{-3} respectively, inside the volcanic plume. This leads to column densities of 1×10^{18} molecules cm^{-2} for SO_2 and 1×10^{14} molecules cm^{-2} for BrO, assuming the light path is

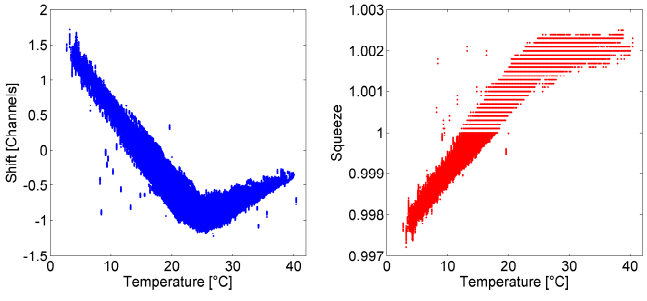

Figure 5. Shift and squeeze for a DOAS fit only containing one reference spectrum with an instrument temperature of 15 °C. For this plot half a year of data were evaluated. It can be clearly seen that the instrument pixel-to-wavelength alignment is influenced by changes in the ambient temperature.

a straight line through the plume centre. The resulting BrO/SO_2 ratio is 1.0×10^{-4}. The instrument was placed below the plume at a height of 4.5 km, and the viewing direction was always directed towards the centre of the volcanic plume. The influence of an increasing distance between instrument and plume has been investigated by varying the lateral distance between 0 km and 6.5 km.

In order to investigate the influence of clouds, we simulated clouds in different heights. Three different cloud layers with heights between 5.5 and 6.5 km (the height of the

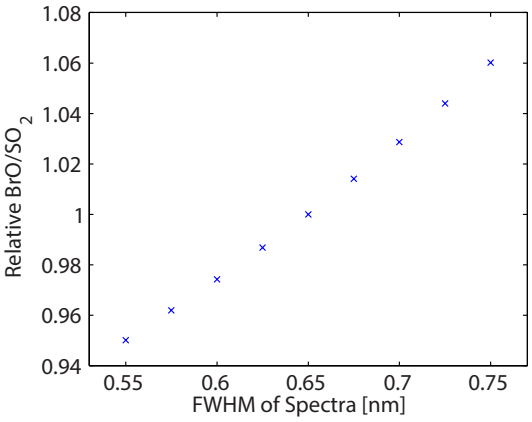

Figure 6. Deviation of the BrO/SO_2 ratio for varying synthetic spectra with different optical resolution. All spectra were evaluated using absorption cross sections that were convolved with a Gaussian profile with a FWHM of 0.65 nm.

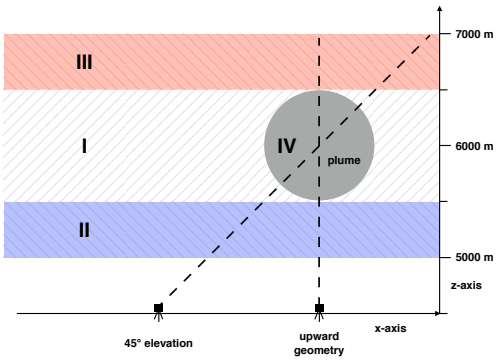

Figure 7. Sketch of the simulated geometries for the McArtim simulations. A round plume with a diameter of 1 km was simulated with the instrument either directly below the volcanic plume or at a horizontal distance. The hatched areas indicate the three different regions in which clouds were simulated. The fourth scenario assumes the absence of clouds but a homogeneous aerosol enhancement inside the volcanic plume (round grey area).

volcanic plume, CS I), 5 and 5.5 km (a cloud layer between the volcanic plume and the instrument, CS 2) and 6.5 and 7 km (a cloud layer above the instrument, CS 3) were simulated. Aerosol with an Ångström exponent of 1, a single scattering albedo of 1 and an asymmetry parameter $g = 0.85$ was used in simulating the cloud (see, e.g. Wagner et al., 2013). Two different aerosol extinction coefficients were simulated to assess variations of the cloud optical depth. The aerosol extinction coefficient was chosen so that the aerosol optical depth for an upward looking instrument was 4.25 and 4 or 12.75 and 12 at 320 and 340 nm, respectively. Additionally as a fourth scenario an enhanced aerosol abundance coinciding with the volcanic plume was simulated. For all cloud simulations only two geometries – an instrument below the volcanic plume with an upward-looking telescope (elevation angle 90°), and an instrument at a lateral distance of 1.5 km with an elevation angle of 45° – were simulated.

3 Results from Nevado del Ruiz

Nevado del Ruiz is a 5400 m high stratovolcano located in the Andes in Colombia, approximately 130 km west of Bogotá. Nevado del Ruiz became infamous in 1985, when on the 13 November approximately 23 000 people were killed by lahars in the aftermath of an eruption. A map showing the location of Nevado del Ruiz and the original two NOVAC instruments whose data are used in this work and their scanning directions are given in Fig. 1.

3.1 Spectroscopy results

Scans between November 2009 and the end of June 2013 were evaluated for two instruments at Nevado del Ruiz, Colombia. Figure 8 shows the number distribution of the BrO DOAS retrieval errors for both instruments (with identification numbers D2J2200 for Bruma and D2J2201 for Alfombrales; see Fig. 1). The fit error is shown for the evaluation of spectra from individual scans as well as for spectra resulting from co-adding four consecutive scans. The DOAS fit errors for the two instruments are essentially equal. For a single scan the fit error is centred around 2×10^{13} molecules cm^{-2}; for the co-added spectra the fit error is centred around 1×10^{13} molecules cm^{-2}. That is, averaging four scans reduces to half the fit error, which indicates that the evaluation is still limited by photon shot noise.

Adding up spectra from different scans is always a trade-off between gaining in signal to noise and losing in absolute signal (for some spectra) and time resolution of the retrieved slant column densities (SCDs). An additional problem may be caused by a drifting spectral instrument response due to changes of the instrument temperature, which would compromise the accuracy of the results when summing up spectra. The variability of the instrument slit function and the wavelength-channel alignment with changing instrument temperature for the spectrometers used in this study is shown in Fig. 5. For this example, one zenith looking spectrum was fitted to spectra from half a year of data with a fit range covering the SO_2 and the BrO evaluation range. Figure 5 shows, as one example, the shift and squeeze of the reference spectrum, which both clearly vary with changes of the ambient temperature.

However, as the signal to noise ratio for four consecutive scans is still close to the ideal photon statistics limited case, the approach to add up spectra from four consecutive scans is thought to not be influenced by these temperature issues and is used in the rest of this manuscript.

SO_2 and BrO column density time series and the SO_2 emission rates are shown in Fig. 9. Both the SO_2 and the BrO column densities start to increase at the beginning of

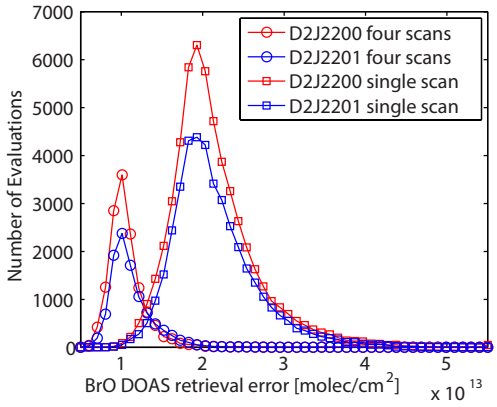

Figure 8. The BrO DOAS fit errors for both instruments whose data are presented in this study. The plot shows the results for spectra from single scans and for spectra co-added from four consecutive scans. The latter have a 50 % lower BrO DOAS fit error than single scans.

2012, as well as the SO_2 emission rates. Towards the beginning of 2013, the SO_2 column densities start to decline while the BrO column densities stay elevated, thus leading to increasing BrO / SO_2 ratios. Unfortunately, both instruments have some periods without transmitted data. D2J2201 has very few scans between July 2011 and November 2011, and the instrument with the serial number D2J2200 has a gap between June 2012 and September 2012. These gaps are due to technical difficulties that can occur when operating the instruments in remote locations. That is, the gap of D2J2200 after June 2012 can be explained by ash from the eruption falling onto the surface of the solar panels, which leads to a lack of power supply.

As there is only a relative small amount of data points ($\sim$ 1–30) per day after the co-addition of scans, the usual approach of calculating the linear regression for a large amount of data points (Bobrowski et al., 2003) to find the BrO / SO_2 ratio cannot be used here. We therefore calculated daily averages of the BrO / SO_2 ratios from the spectra created from co-adding four consecutive scans for the sake of lower noise. Averaging over all ratios can lead to erroneous results, since the average would include many scans without significant volcanic gas and therefore negligible SO_2 and BrO column densities. Taking the ratio of two values (i.e. SO_2 and BrO SCDs) that are close to zero gives unpredictable and unrealistic results. Therefore, SCDs measured outside the volcanic plume have to be excluded. One possibility is setting a BrO threshold equivalent to a certain factor of the retrieval error as a BrO detection limit. An example of a time series created for all scans containing BrO above the detection limit (in this case 4 times the retrieval error was chosen) is shown in Fig. 10. The BrO / SO_2 ratio is almost constant between January 2011 and January 2012 with a value of roughly 6–8×10^{-5}. Starting January 2012, the ratio drops down to values as low as 2×10^{-5}, and increases again up to 4×10^{-5} after an eruption on 30 June 2012 (vertical bar in Fig. 10). However, this approach is problematic since BrO is often close to the detection limit. In this case, setting a BrO threshold would remove low BrO values, and thus lead to elevated BrO / SO_2 ratios.

In this work we therefore chose to set an SO_2 threshold of 7×10^{17} molecules cm^{-2} to select spectra for the evaluation of the BrO / SO_2 ratio. This threshold is a relatively high SO_2 column density. However for the lower values of the BrO / SO_2 ratio in Fig. 10 ($\sim 2 \times 10^{-5}$) this would result in a BrO column density as low as 1.4×10^{13} molecules cm^{-2}, a value only slightly higher than the average DOAS retrieval error for BrO. This approach assures that scans not seeing significant amounts of volcanic gas are filtered out and thus will not significantly influence the BrO / SO_2 ratio. The result is shown in the middle of Fig. 10; the BrO / SO_2 ratio is again constant until January 2012 but with a lower value of 4×10^{-5}. In 2012 there is a drop before the ratio increases again up to 4×10^{-5} after the eruption. Towards the end of 2012, the ratio sinks until the end of June 2013 (no more data were available at the time of this manuscript).

The trends found in the BrO / SO_2 molar ratios are similar irrespective of the thresholds chosen for the calculation of the mean BrO / SO_2 ratio. Interestingly, they show a clear correspondence with the general evolution of the volcanic activity, as expressed by the levels of risks defined by the authorities. The decrease in the measured BrO / SO_2 ratio starts a few months before the main eruptive event that led to a rise of the alert to the highest (red) level.

After the eruption the BrO / SO_2 ratio recovers again, when the level of activity decreases. Many causes can produce the observed pattern in the BrO / SO_2 molar ratio, as for example the injection of an SO_2-rich batch of magma, or atmospheric effects like a different depletion rate of the two species due to scavenging by aerosols and ash in the plume. Garzon et al. (2013) suggested that the time between 30 March 2012 and 30 May 2012 was dominated by magma intrusion processes and had high sulfur emissions as well as first ash emissions (see Fig. 9 for daily averages of the SO_2 emission rates). Although a detailed analysis of this process is beyond the scope of this paper, the correspondence with the overall eruptive activity shows the potential of measuring both gases simultaneously as a precursory signal of volcanic eruptions.

3.2 The influence of radiative transfer

The results of the radiative transfer model calculations for an increasing lateral distance between instrument and plume (without any clouds) are shown in Figs. 11 and 12. Figure 11 shows the decline of the SO_2 and BrO CDs. At a distance of 6.5 km, only 75 % of the SO_2 CD and and 78 % of the BrO CD are retrieved. However, the variation of the BrO/SO_2 ratio is significantly lower (see Fig. 12). Even at a lateral distance of 6.5 km, the BrO/SO_2 ratio is only $\approx$ 6 % above the

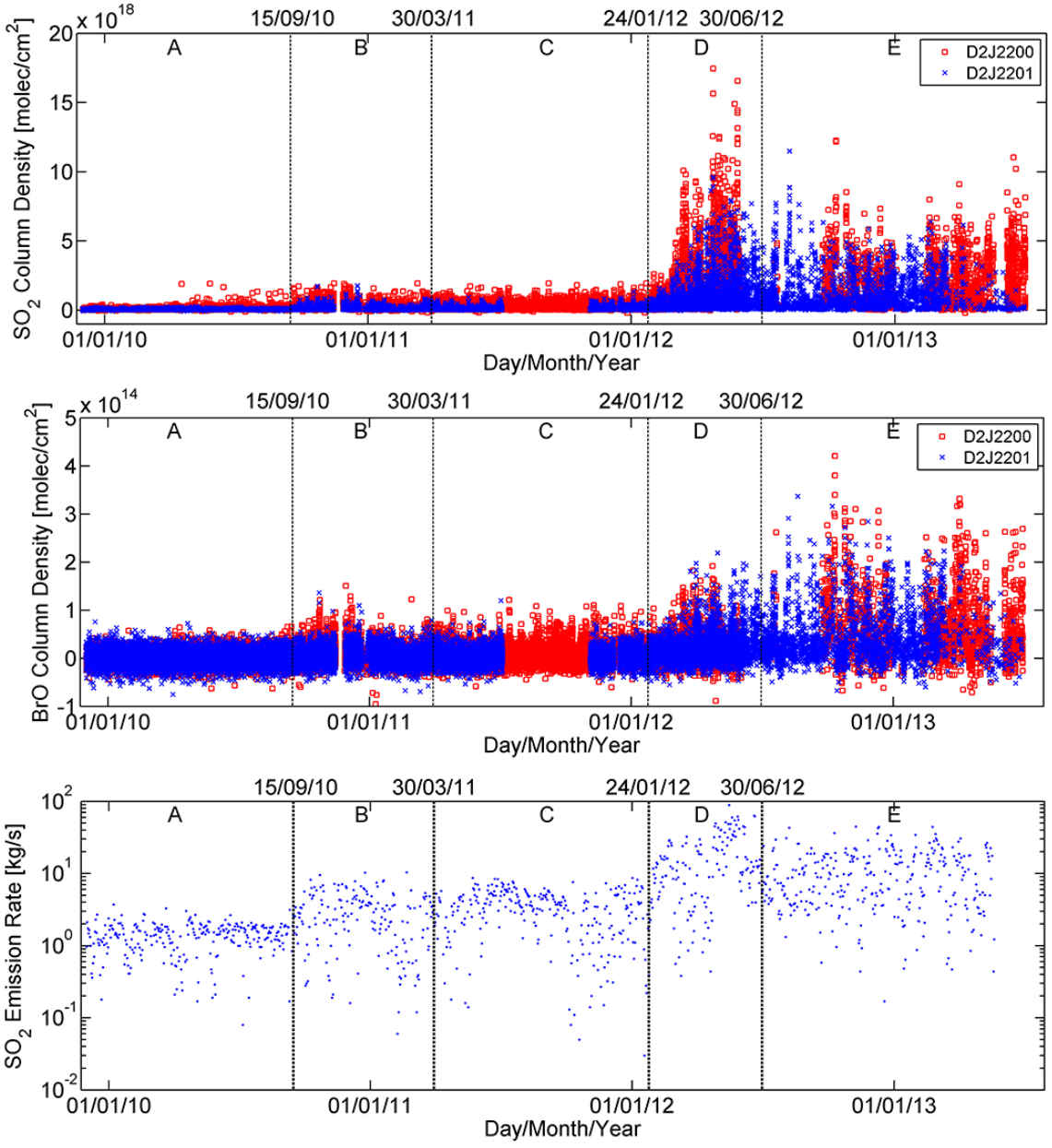

Figure 9. Time series from the two instruments at Nevado del Ruiz. The instrument D2J2200 is located in a way that measures elevated SO_2 and BrO column density values more frequently (see Fig. 1). The spectra evaluated were created from co-adding reference and plume spectra from four consecutive scans. Top: SO_2 CDs; centre: BrO CDs; bottom: Daily averages of the SO_2 emission rates. The wind speed was taken from the ECMWF database. More details are available in Galle et al. (2010) and Arellano (2013).

true value. Generally speaking, the slight overestimation of the BrO/SO_2 ratio arises from the fact that the light dilution effect leads to a decrease of the detected CDs and is more pronounced at smaller wavelengths. The situation is more complex in reality. The light-dilution effect depends on the wavelength as well as on the optical density of the absorber. However, these simulations show that the influence of light dilution is smaller for the ratio of trace gases than for the CDs.

The results for the different clouds scenarios are shown in Table 1 (aerosol optical depth, AOD = 4 at 340 nm for an upward-looking instrument) and Table 2 (AOD = 12 at 340 nm for an upward-looking instrument). We can see that a cloud at the same height as the volcanic plume (CS I and CS IV) leads to larger trace gas column densities (up to 40 % overestimation depending on viewing geometry and AOD). However, the BrO/SO_2 ratio is retrieved correctly within 2.4 %. The largest deviations can be observed for a cloud

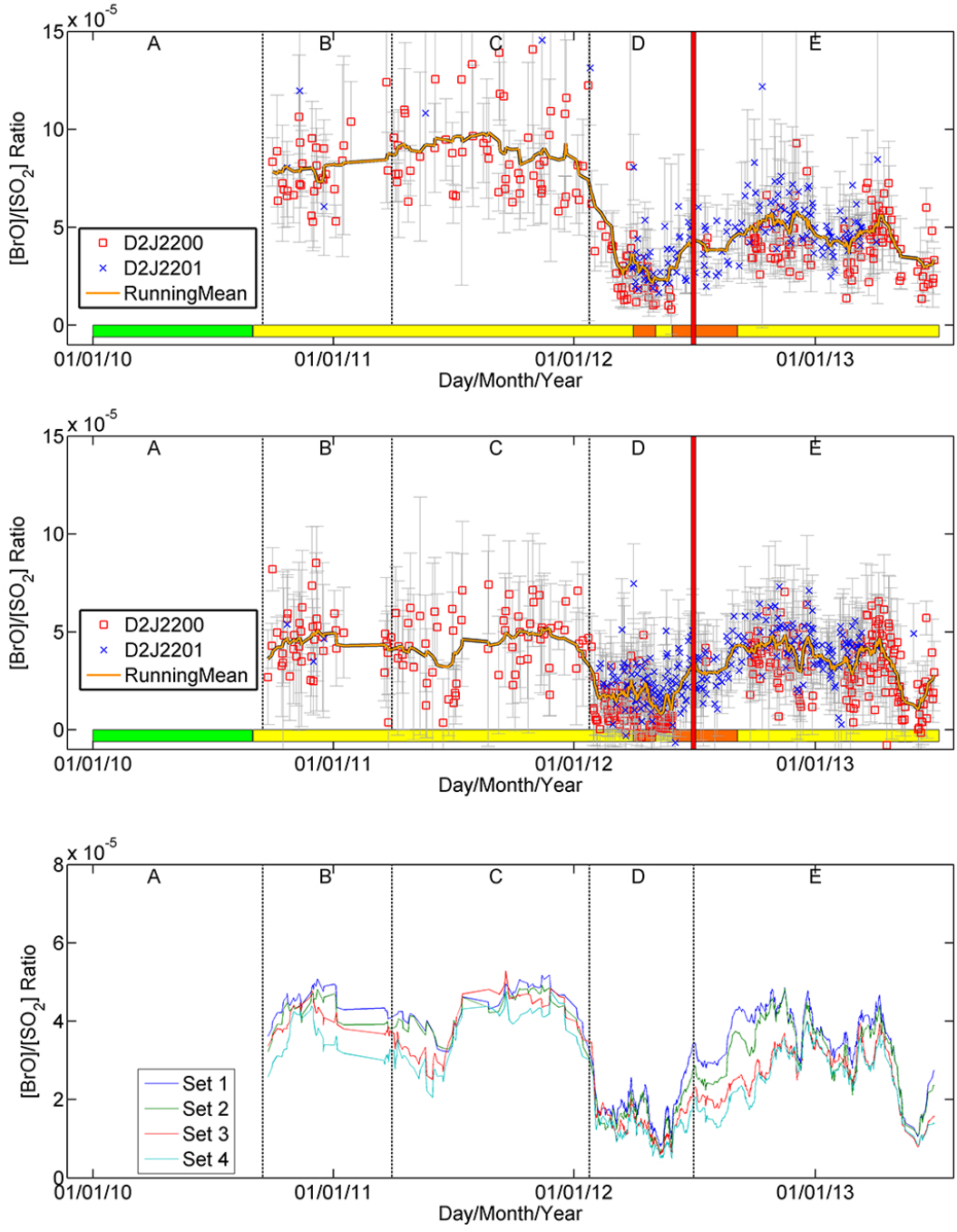

Figure 10. Daily averages of the BrO/SO_2 molar ratios from Nevado del Ruiz from November 2009 to June 2013. The ratio drops down to values below 5×10^{-5}, and increases again after the eruption on 30 June 2012 (red vertical bar). Also shown at the bottom of the image is the volcanic activity risk level defined by the Colombian Geological Survey (coloured horizontal bars). The black-orange line shows a running mean around seven data points (from both instruments). Top: the criterion for a valid measurement is a BrO column density above four times the BrO DOAS retrieval error. Center: for this figure an SO_2 threshold of 7×10^{17} molecules cm^{-2} was chosen as the criterion for valid data points. Bottom: Running mean of the BrO/SO_2 time series retrieved in different wavelength ranges, with an SO_2 threshold of of 7×10^{17} molecules cm^{-2} as the criterion for valid data points.

below the volcanic plume. For an instrument with an elevation angle of 45°, the true CDs are underestimated by up to 80 %. However, even in these conditions the deviation of the BrO/SO_2 ratio is below 3.5 %. This shows that the BrO/SO_2 ratio is much more robust with regards to radiative transfer

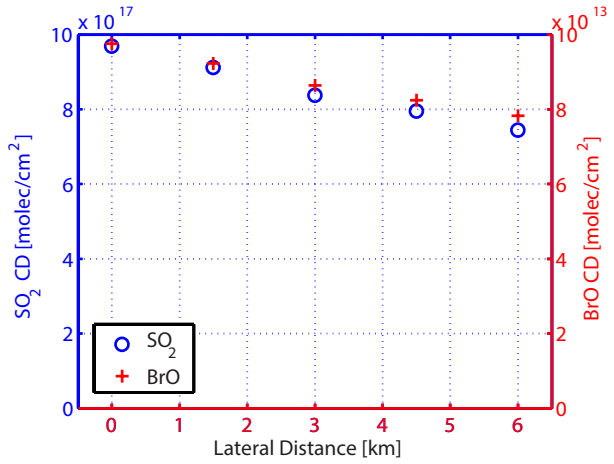

Figure 11. The influence of an increasing lateral distance between instrument and plume on the SO_2 and BrO CDs. For all calculations the volcanic plume was simulated 1.5 km above the instrument. The SO_2 column densities were simulated at 320 nm, the BrO column densities at 340 nm.

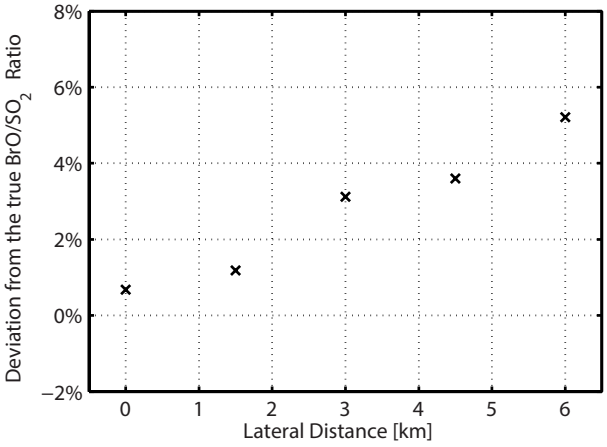

Figure 12. McArtim results for the influence of an increasing lateral distance between instrument and volcanic plume on the SO_2/BrO ratio. The ratio of the two trace gases is only slightly influenced by an increasing distance.

issues than individual SO_2 or BrO CDs, as one would expect intuitively.

As an additional verification step for the retrieved BrO/SO_2 ratios, both trace gases were evaluated in different wavelength ranges. As the alternative SO_2 evaluation range (326.8–353.5 nm) does not contain the strong SO_2 absorption bands, the DOAS fit error was found to be roughly 10 times higher than in our standard range. We found good correlation between the SO_2 CDs retrieved in the two evaluation ranges. The SO_2 CDs in the alternative wavelength range are $\approx 30\,\%$ higher than in the standard wavelength range. However, the alternative evaluation range should be treated with care because of the greater instability of the fitting algorithm due to the lower absorption of SO_2.

The BrO CDs retrieved in the two evaluation ranges are generally the same. The BrO fit error in the alternative wavelength range (327–347 nm) was found to be $\approx 30\,\%$ higher than in the standard range.

Time series of the BrO/SO_2 ratio were created for all combinations of the different wavelength ranges:

- *Set 1* SO_2: 314.8–326.8 nm, BrO: 330.6–352.75 nm; this are the standard evaluation ranges used in the rest of this work
- *Set 2* SO_2: 314.8–326.8 nm, BrO: 327–347 nm
- *Set 3* SO_2: 326.8–353.5 nm, BrO: 330.6–352.75 nm
- *Set 4* SO_2: 326.8–353.5 nm, BrO: 327–347 nm

For a clearer presentation only the running mean values for the four sets are shown at the bottom of Fig. 10. The same general trend is observed for all evaluation ranges, with a tendency of higher BrO/SO_2 ratios for set 1 and 2. These observations follow the previous findings on the effect of different evaluation ranges for SO_2. Evaluating SO_2 at larger wavelengths leads to higher CDs for two reasons: the influence of the light-dilution effect is lower at larger wavelengths, and the DOAS retrieval is less influenced by non-linearities that can occur for strong absorbers. The larger SO_2 CDs lead to lower BrO/SO_2 ratios when evaluating SO_2 in the alternative wavelength range.

3.3 Comparison with geophysical data and observations

We compared our obtained time series of BrO/SO_2 ratios with seismic activities as reported in Herrick (2012) and in the technical reports of the SGC – Servicio Geológico Colombiano[1] (formerly INGEOMINAS). Based on the SO_2 emission rate and number of volcano-tectonic (VT) and long-period (LP) seismic events, we divided the observation period in five different intervals.

In the first interval (A) between November 2009 (when the instruments where first installed) until mid-September 2010, we observe low average daily SO_2 emission rates below $3\,\mathrm{kg\,s^{-1}}$. Gas emissions are too low to successfully retrieve BrO/SO_2 ratios. At the same time seismic activity (see Figs. 13 and 14) is very low, and the national park was open for tourists visiting Nevado del Ruiz.

Interval B, between mid-September 2010 and end of March 2011, is characterized by higher SO_2 emission rates up to $10\,\mathrm{kg\,s^{-1}}$. Gas emissions are high enough to retrieve BrO/SO_2 ratios with an average value of $\approx 5 \times 10^{-5}$. The number of VT and LP events per month increases by an order of magnitude. At 6:30 a.m. on 5 November 2010, a first high volcanic column with a height of 900 m was reported by neighbours located more than 50 km from Nevado del Ruiz. On 11 December 2010 a first explosion was registered in the

[1] http://www.sgc.gov.co/lastaccessed:28.02.2014.

Table 1. SO_2 CDs, BrO CDs and the BrO/SO_2 ratios for the different cloud scenarios and a cloud optical density of 4 at 340 nm. (0) is a cloud-free atmosphere, (I) a cloud layer between 5.5 and 6.5 km, (II) a cloud layer between 5 and 5.5 km, (III) a cloud layer between 6.5 and 7 km, and (IV) an enhanced aerosol abundance coinciding with the volcanic plume.

		SO_2 [molec/cm^2] $\times 10^{18}$	BrO $\times 10^{14}$	BrO/SO_2 ratio $\times 10^{-4}$	Deviation [%]
0	90°	0.97	0.98	**1.006**	0.6
	45°	0.92	0.93	**1.014**	1.4
I	90°	1.09	1.09	**1.000**	0.0
	45°	1.04	1.05	**1.013**	1.3
II	90°	0.95	0.97	**1.028**	2.8
	45°	0.28	0.27	**0.976**	−2.5
III	90°	0.96	0.96	**1.000**	0.0
	45°	1.01	1.02	**1.008**	0.8
IV	90°	1.08	1.08	**0.999**	−0.1
	45°	1.07	1.09	**1.013**	1.3

Table 2. SO_2 CDs, BrO CDs and the BrO/SO_2 ratios for the different cloud scenarios and a cloud optical density of 12 at 340 nm. (0) is a cloud free atmosphere, (I) a cloud layer between 5.5 and 6.5 km, (II) a cloud layer between 5 and 5.5 km, (III) a cloud layer between 6.5 and 7 km, and (IV) a cloud layer coinciding with the volcanic plume.

		SO2 [molec/cm^2] $\times 10^{18}$	BrO $\times 10^{14}$	BrO/SO2 ratio $\times 10^{-4}$	Deviation [%]
0	90°	0.97	0.98	**1.006**	0.6
	45°	0.92	0.93	**1.014**	1.4
I	90°	1.37	1.36	**0.997**	−0.3
	45°	1.17	1.20	**1.023**	2.3
II	90°	0.81	0.83	**1.034**	3.4
	45°	0.22	0.22	**0.996**	−0.4
III	90°	0.99	0.99	**0.999**	−0.1
	45°	1.03	1.04	**1.006**	0.6
IV	90°	1.26	1.26	**0.999**	−0.1
	45°	1.20	1.22	**1.024**	2.4

centre of the active Arenas crater of Nevado del Ruiz at 12:51 local time.

Interval C, between April 2011 and mid-January 2012, shows SO_2 emission rates and BrO/SO_2 ratios similar to interval B. The number of LP events stays similar as well, but the number of monthly VT events drops to approximately half of the number in interval B. On 21 August 2011 another relatively high volcanic column with a height of 900 m was observed on the top of Nevado del Ruiz volcano. This period was accompanied by small explosions and some glacier avalanches around the main active Arenas crater.

Interval D starts at the beginning of February 2012 and ends with the explosion of Nevado del Ruiz on 30 June 2012. The SO_2 emission rate is generally largely increased with maximum values of the daily average emission rate up to 88 kg s^{-1}. In this interval the BrO/SO_2 ratio drops to lower values $\approx 1-2\times10^{-5}$. At this time the number of VT events reaches similar values to interval B and the number of monthly LP events increases by an order of magnitude. Ash emissions were observed at the end of February (Garzón et al., 2013). The time between March and May 2012 was described as dominated by magma intrusion processes by Garzón et al. (2013).

Interval E starts after the explosion on 30 June and lasts till the end of our observations. The SO_2 emission rates slightly decrease (maximum daily averages of 45 kg s^{-1}), and the BrO/SO_2 ratio recovers to values of $\approx 5\times10^{-5}$. However, another drop of the BrO/SO_2 ratio can be observed from mid-April 2013 until the end of our observations (June 2013). The number of LP events is lower again, similar to periods B and C. The number of VT events is characterized by high variations. The highest number of VT events coincides with another decrease of the BrO/SO_2 ratio. During this period ash emissions can be observed occasionally.

We can summarize that there are changes of the BrO/SO_2 ratio that coincide with variations of seismic signals. At the

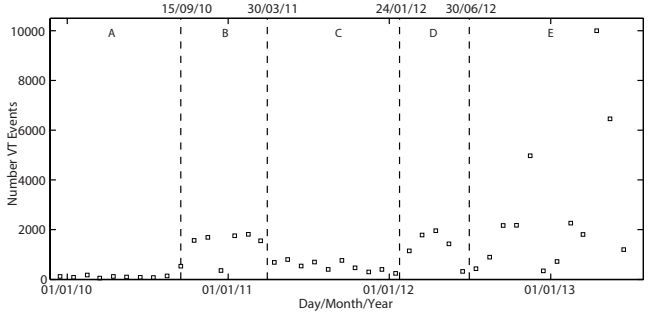

Figure 13. Number of volcano tectonic events per month. Data are taken from the SGC reports from http://www.sgc.gov.co/.

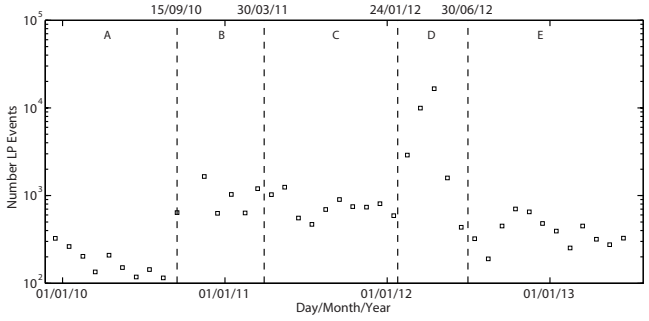

Figure 14. Number of long period seismic events per month. Data are taken from the SGC reports from http://www.sgc.gov.co/.

same time as the first drop of the BrO/SO_2 ratio (Interval D), the SGC reports indicate a large increase in the number of LP events. During the second drop of the BrO/SO_2 ratio, the number of VT events increases.

A robust interpretation of the observed BrO/SO_2 ratios is difficult with our current knowledge. Only few measurements of solubility of bromine have been carried out (e.g. Villemant and Boudon, 1999, Bureau et al., 2000, and 2010, Balcone-Boissard et al., 2010). No information can be found whether bromine exsolves from the magma earlier than sulfur. We therefore briefly discuss both possibilities. Assuming that bromine exsolves later than sulfur, we could identify interval B and C as a system in some kind of intermediate equilibrium with a BrO/SO_2 ratio of $\approx 5 \times 10^{-5}$. In case of a pressure decrease, we then expect first a decrease in the BrO/SO_2 ratio caused by the exsolution of sulfur. If the pressure decreases further at a certain point, bromine becomes exsolved as well and the BrO/SO_2 increases again, which can be observed in the data at the transition between intervals D and E.

However, the observed pattern can also be interpreted reasonably assuming that bromine exsolves from the magma before sulfur as suggested in Bobrowski and Giuffrida (2012). In this case we would expect an increase in bromine emissions (and therefore of the BrO/SO_2 ratio) when the pressure starts to decrease. This cannot be excluded nor confirmed from our data set. The BrO/SO_2 ratio could have increased in interval A, where general gas emissions were too low to exceed the detection limit. Small increases of the BrO/SO_2 ratio can be observed at the beginning of interval B and in the middle of interval C. We can also not exclude (with our time resolution) that an increase of the BrO/SO_2 ratio was too fast to be detected. The seismic signals already indicate changes of the volcanic system in interval B and C. As the pressure decreases further (Interval D), a relatively larger fraction of sulfur exsolves from the magma. As magma generally contains more sulfur than bromine, this leads to a decrease of the BrO/SO_2 ratio.

Another factor affecting the relative speciation of BrO/SO_2 in the plume is the effect of magma ascent rate on the efficiency of segregation of volatile species. Balcone-Boissard et al. (2010) found that for felsic magmas Cl, Br and I are extracted efficiently at high pressure during slow magma ascent, but remained in the melt during explosive degassing. Although the magmatic composition of Nevado del Ruiz is not felsic, a similar dynamical effect could be present in this volcano. The drop in the BrO/SO_2 ratio preceding the explosive phase of the eruption may thus indicate acceleration of the magma from the reservoir, affecting in different ways the exsolution of the two species.

4 Discussion of results and outlook

We have for the first time demonstrated that BrO column densities can be automatically evaluated from spectra routinely recorded by the NOVAC type 1 instruments of the NOVAC network. This proof of concept shows the possibility of achieving a 5-year or even longer time series of BrO/SO_2 ratios at many (if not all) volcanoes observed by the NOVAC network. The instruments with which the data were analysed in this study have exactly the same design as any other NOVAC type 1 instrument. In fact 2 years of data (January 2011–December 2012) at Galeras, Colombia, were also evaluated. While in general showing too low SO_2 levels for a successful BrO detection, the BrO DOAS retrieval error was comparable to the error from the instruments at Nevado del Ruiz. Since Nevado del Ruiz was chosen for this study due to the interesting activity and the good continuous data set, not for superior instrument performance, we have no indications that the other instruments from NOVAC should perform differently. Furthermore, there are other networks (i.e. the Flame network at Stromboli, Italy; Burton et al., 2009) that use comparable spectrometers, which could give further insight into volcanic BrO/SO_2 ratios. Evaluating BrO and SO_2 in different wavelength ranges and radiative transfer calculations showed that the BrO/SO_2 ratio is more robust against influences of radiative transfer than the trace-gas column densities.

The large NOVAC data set already gives the possibility to determine other influences than changes of the volcanic

activity on the BrO/SO_2 molar ratio. BrO is not primarily emitted by volcanoes but forms from HBr when volcanic gases are released into the atmosphere (e.g. Bobrowski et al., 2003; Oppenheimer et al., 2006, von Glasow, 2010). While this potentially makes it more difficult to use the BrO/SO_2 ratio as an indicator of volcanic activity, Bobrowski and Giuffrida (2012) have found that the BrO/SO_2 molar ratio increases only in the first minutes after release into the atmosphere. The authors found that, at a distance of approximately 5 km after release into the atmosphere, the BrO/SO_2 molar ratio is constant (of course depending on the wind speed). The vast amount of available data in the NOVAC database allows the further investigation of influences like the residence time of the volcanic gas in the ambient atmosphere by estimating the time of transport from the volcanic vent to the point of measurement, or meteorological influences on the BrO/SO_2 molar ratio, as well as its dependence on height and latitude.

The BrO evaluation scheme presented in this manuscript was implemented for automatic operation to re-process the archived data. In the future, it is planned to be implemented into the routine evaluation for the NOVAC observatories. Besides the automated evaluation there are chances to further improve the quality of the BrO/SO_2 ratios.

One possible pitfall in the DOAS evaluation of volcanic gas measurements is the requirement of a reference spectrum free of volcanic gas. For instance, this problem is discussed in Salerno et al. (2009), where the authors state that wide volcanic gas plumes, covering the complete range of viewing directions, are frequently observed. This problem is probably most frequently observed during periods of low wind speeds, when meaningful gas emission rate measurements are difficult anyways. Therefore, it is not the main concern for SO_2 emission rate measurements. However, using gas-free reference spectra can improve the BrO retrieval. An approach similar to that described by Salerno et al. (2009) for the evaluation of SO_2 without a reference spectrum could be implemented. The background spectrum for the evaluation is modelled on the basis of an extraterrestrial solar reference spectrum (Chance and Kurucz, 2010). Unfortunately, while working well for volcanic SO_2, the approach of using modelled spectra does not yield sufficient accuracy for the BrO evaluation at this time.

However, this method could be used to identify "plume-free" spectra, by their SO_2 signatures, which subsequently can be used as reference spectra to evaluate the data for both BrO and SO_2. If all spectra from a particular scan of the sky contain significant SO_2 column densities, one could, for example, use a reference spectrum from a different scan or day, with similar atmospheric conditions and a similar instrument temperature.

Another possible approach to further improve the accuracy of our algorithm is taking temperature effects of the instruments, which were discussed in the Methods section, into account. This could further help to improve the quality of data evaluation.

The results presented in this work are – although there is still ample potential for improvements – encouraging and show that data recorded by NOVAC can be used to routinely perform measurements of the BrO/SO_2 molar ratio as an additional tracer of volcanic activity. The sample data set presented here already demonstrates that the BrO/SO_2 showed significant changes several weeks prior to major eruptive events. The variations of the BrO/SO_2 ratio occur at a similar time as increased seismic activity. If BrO/SO_2 ratios could be considered as an additional indicator of changes in the volcanic activity, even earlier warnings and discussion about potential risk could be initiated. However, more data are necessary to confirm this behaviour – but they might be soon available considering the large database of NOVAC.

Acknowledgements. The authors would like to thank Mike Burton for editing and two anonymous reviewers for their comments on the manuscript, which greatly helped to improve it. We would like to thank the European Commission Framework 6 Research Program for funding of the NOVAC project. We kindly acknowledge the NOVAC partners from the Colombian Geological Survey (formerly INGEOMINAS), especially the FISQUIM Research Group and the technical staff at the Manizales Volcanological Observatory, which permanently works for the maintenance of the energy supply for the ScanDOAS systems located around the main crater of Nevado del Ruiz volcano. The authors would like to thank Tim Deutschmann for providing the radiative transfer model McArtim. N. Bobrowski thanks for financial support from the DFG project DFG BO 3611/1-1. The authors thank the DFG project DFG PL 193/14-1 for financial support.

The service charges for this open access publication have been covered by the Max Planck Society.

Edited by: M. Burton

Appendix A:

We simulated synthetic spectra as outlined in Vogel (2011). Measurement and Fraunhofer reference spectra (FRS) were both simulated. The BrO content of the measurement spectrum was 1.5×10^{14} molecules cm^{-2}, and the SO_2 content was 1×10^{18} molecules cm^{-2}. The synthetic spectra are based on the Chance and Kurucz (2011) solar atlas. The Beer–Lambert law was applied on the wavelength grid of the solar atlas using stratospheric absorbers and in the case of the measurement spectrum additionally BrO and SO_2. Then the high-resolution spectra were convolved to a lower resolution with a Gaussian profile with varying FWHM. The FWHM was varied between 0.525 and 0.775 nm in steps of 0.025 nm. For each FWHM a set of measurement and FRS spectrum (convolved with the same Gaussian profile) were evaluated using the DOAS retrieval as outlined in the Methods section. The absorption cross sections were convolved with a Gaussian profile with a FWHM of 0.65 nm. This approach mimics the situation in NOVAC. While a constant FWHM is used for the convolution of the absorption cross sections, the instrument line shape of both spectra varies with temperature. Figure 6 shows the deviation of the BrO/SO_2 ratio from the BrO/SO_2 ratio retrieved with both spectra using the same instrument line shape. The results show that the error in the BrO/SO_2 ratio is below 15 % for variations of the instrument line shape of up to 0.125 nm.

References

Arellano, S. R.: Studies of Volcanic Plumes with Spectroscopic Remote Sensing Techniques, Licentiate thesis, Chalmers University of Technology, Göteborg, Sweden, 2013.

Balcone–Boissard, H., Villemant, B. and Boudon, G.: Behavior of halogens during the degassing of felsic magmas, Geochem. Geophy. Geosy., 11, Q09005, doi:10.1029/2010GC003028, 2010.

Bobrowski, N. and Giuffrida, G.: Bromine monoxide/sulphur dioxide ratios in relation to volcanological observations at Mt. Etna 2006–2009, Solid Earth, 3, 433–445, 2012.

Bobrowski, N. and Platt, U.: SO_2/BrO ratios studied in five volcanic plumes, J. Volcanol. Geoth. Res., 166, 147–160, 2007.

Bobrowski, N., Hönninger G., Galle, B., and Platt, U.: Detection of bromine monoxide in a volcanic plume, Nature, 423, 273–276, 2003.

Boichu, M., Oppenheimer, C., Roberts, T. J., Tsanev, V., and Kyle, P. R.: On bromine, nitrogen oxides and ozone depletion in the tropospheric plume of Erebus volcano (Antarctica), Atmos. Environ., 45, 3856–3866, 2011.

Bureau, H., Keppler, H. and Métrich, N.: Volcanic degassing of bromine and iodine: experimental fluid/melt partitioning data and applications to stratospheric chemistry, EARTH PLANET SC LETT, 183, 51–60, 2000.

Bureau, H., Foy, E., Raepsaet, C., Somogyi, A., Munsch, P., Simon, G., and Kubsky, S.: Bromine cycle in subduction zones through in situ Br monitoring in diamond anvil cells, GEOCHIM COSMOCHIM AC, 74, 3839–3850, 2010.

Burrows, J. P., Richter, A., Dehn, A., Deters, B., Himmelmann, S., Voigt, S., and Orphal, J.: Atmospheric remote-sensing reference data from GOME-2. Temperature-dependent absorption cross sections of O_3 in the 231–794 nm range. J. Quant. Spectrosc. Ra., 61, 509–517, 1999.

Burton, M. R., Caltabiano, T., Murè, F., Salerno, G., and Randazzo, D.: SO_2 flux from Stromboli during the 2007 eruption: results from the FLAME network and traverse measurements, J. Volcanol. Geoth. Res., 182, 214–220, 2009.

Carroll, M. R. and Holloway, J. R.: Volatiles in Magmas, Mineralogical Society of America, Washington DC, 517 pp., 1994.

Chance, K. and Kurucz, R. L.: An improved high-resolution solar reference spectrum for earth's atmosphere measurements in the ultraviolet, visible, and near infrared, J. Quant. Spectrosc. Ra., 111, 1289–1295, 2010.

Deutschmann, T., Beirle, S., Fried, U., Grzegorski, M., Kern, C., Kritten, L., Platt, U., Prados-Román, C., Puckite, J., Wagner, T., Werner, B., and Pfeilsticker, K.: The Monte Carlo atmospheric radiative transfer model McArtim: Introduction and validation of Jacobians and 3D features, Journal of Quantitative Spectroscopy and Radiative Transfer, 112, 1119–1137, 2011.

Fleischmann, O. C., Hartmann, M., Burrows, J. P., and Orphal, J.: New ultraviolet absorption cross-sections of BrO at atmospheric temperatures measured by time-windowing Fourier transform spectroscopy, J. Photoch. Photobio. A, 168, 117–132, 2004.

Galle, B., Oppenheimer, C., Geyer, A., McGonigle, A. J. S., Edmonds, M., and Horrocks, L.: A miniaturised ultraviolet spectrometer for remote sensing of SO_2 fluxes: a new tool for volcano surveillance, J. Volcanol. Geoth. Res., 119, 241–254, 2003.

Galle, B., Johannson, M., Rivera, C., Zhang, Y., Kihlmann, M., Kern, C., Lehmann, T., Platt, U., Arellano, S., and Hidalgo, S.: Network for Observation of Volcanic and Atmospheric Change (NOVAC) – a global network for volcanic gas monitoring: Network layout and instrument description, B. Volcanol., 115, D05304, doi:10.1029/2009JD011823, 2010.

Garzon, G., Silva, B., Narvaez, A., Chacon, Z., and Galle, B.: Assessment of SO_2 emissions from three Colombian active volcanoes (2007–2012), GEOCHANGE: Problems of Global Changes of the Geological Environment, vol. 2, edited by: Khalilov, E., Science Without Borders, London, 6–14, 2013.

Grainger, J. F. and Ring, J.: Anomalous Fraunhofer line profiles, Nature, 193, 762, doi:10.1038/193762a0, 1962.

Hermans, C., Vandaele, A. C., Fally, S., Carleer, M., Colin, R., Coquart, B., Jenouvrier, A., Merienne, M.-F.: Absorption cross-section of the collision-induced bands of oxygen from the UV to the NIR, in: Weakly Interacting Molecular Pairs: Unconventional Absorbers of Radiation in the Atmosphere, edited by: Camy-Peyret, C. and Vigasin, A., Springer, Netherlands, 193–202, 2003.

Herrick, J., Bulletin of the Global volcanism Network (August 2012), vol. 37, 8. last accessed on 27 Nov 2013 from http://www.volcano.si.edu/reports_bgvn.cfm, 2012.

Hörmann, C., Sihler, H., Bobrowski, N., Beirle, S., Penning de Vries, M., Platt, U., and Wagner, T.: Systematic investigation of bromine monoxide in volcanic plumes from space by using the GOME-2 instrument, Atmos. Chem. Phys., 13, 4749–4781, doi:10.5194/acp-13-4749-2013, 2013.

Kelly, P. J., Kern, C., Roberts, T. J., Lopez, T., Werner, C., and Aiuppa, A.: Rapid chemical evolution of tropospheric volcanic emissions from Redoubt Volcano, Alaska, based on observations of ozone and halogen-containing gases, J. Volcanol. Geoth. Res., 259, 317–333, 2012.

Kern, C.: Spectroscopic measurements of volcanic gas emissions in the ultra-violet wavelength region, Ph.D. Thesis, Institute of Enviromental Physics, University of Heidelberg, 2009.

Kraus, S.: DOASIS, A Framework Design for DOAS, Ph.D. Thesis, University of Mannheim, 2006.

Meller, R. and Moortgat, G. K.: Temperature dependence of the absorption cross sections of formaldehyde between 223 and 323 K in the wavelength range 225–375 nm, J. Geophys. Res-Atmos., 105, 7089–7101, 2000.

Menyailov, I. A.: Prediction of eruptions using changes in composition of volcanic gases, B. Volcanol., 39, 112–125, 1975.

Noguchi, K. and Kamiya, H.: Prediction of volcanic eruption by measuring the chemical composition and amounts of gases, B. Volcanol., 26, 367–378, doi:10.1007/BF02597298, 1963.

Oppenheimer, C., Tsanev, V. I., Braban, C. F., Cox, R. A., Adams, J. W., Aiuppa, A. Bobrowski, N., Delmelle, P., Barclay, J., and McGonigle, A. J. S.: BrO formation in volcanic plumes, Geochim. Cosmochim. Ac., 70, 2935–2941, 2006.

Pennisi, M. and Le Cloarec, M.-F.: Variations of Cl, F, and S in Mount Etna's plume, Italy, between 1992 and 1995, J. Geophys. Res-Sol Ea., 103, 5061–5066, 1998,.

Pinardi, G., Roozendael, M. V., and Fayt, C.: The influence of spectrometer temperature variability on the data retrieval of SO2., In NOVAC second annual activity report, NOVAC consortium, 44–48, 2007.

Platt, U. and Stutz, J.: Differential Optical Absorption Spectroscopy – Principles and Applications, Physics of Earth and Space Environments, 1st Edn., Springer, Berlin, Heidelberg, New York, 597 pp., 2008.

Salerno, G. G., Burton, M. R., Oppenheimer, C., Caltabiano, T., Tsanev, V. I., and Bruno, N.: Novel retrieval of volcanic SO_2 abundance from ultraviolet spectra, J. Volcanol. Geoth. Res., 181, 141–153, 2009.

Vandaele, A. C., Hermans, C., Simon, P. C., Carleer, M., Colin, R., Fally, S., Merienne, M., Jenouvrier, A., and Coquart, B.:, Measurements of the NO_2 absorption cross-section from 42 000 cm^{-1} to 10 000 cm^{-1}(238–1000 nm) at 220 K and 294 K, J. Quant. Spectrosc. Ra., 59, 171–184, 1998.

Vandaele, A. C., Hermans, C., and Fally, S.: Fourier transform measurements of SO_2 absorption cross sections: I I.: Temperature dependence in the 29 000–44 000 cm^{-1} (227–345 nm) region, J. Quant. Spectrosc. Ra., 110, 2115–2126, 2009.

Villemant, B. and Boudon, G.: H_2O and halogen (F, Cl, Br) behaviour during shallow magma degassing processes, EARTH PLANET SC LETT, 168, 271–286, 1999.

Vogel, L.: Volcanic plumes: Evaluation of spectroscopic measurements, early detection and bromine chemistry, Ph.D. thesis, Ruperto Carola University of Heidelberg, Germany, available at: http://www.ub.uni-heidelberg.de/archiv/13219, 2011.

Vogel, L., Sihler, H., Lampel, J., Wagner, T., and Platt, U.: Retrieval interval mapping: a tool to visualize the impact of the spectral retrieval range on differential optical absorption spectroscopy evaluations, Atmos. Meas. Tech., 6, 275–299, 2013, http://www.atmos-meas-tech.net/6/275/2013/.

von Glasow, R.: Atmospheric chemistry in volcanic plumes, P. Natl. Acad. Sci. USA, 107, 6594–6599, 2010.

Wagner, T., Chance, K., Frieß, U., Gil, M., Goutail, F., Hönninger, G., Johnston, P., Karlsen-Tørnkvist, K., Kostadinov, I., Leser, H., Petritoli, A., Richter, A., Van Roozendael, M., and Platt, U.: Correction of the ring effect and I0 effect for DOAS observations of scattered sunlight, ESA Technical Report, 2002.

Wagner, T., Beirle, S., and Deutschmann, T.: Three-dimensional simulation of the Ring effect in observations of scattered sun light using Monte Carlo radiative transfer models, Atmos. Meas. Tech., 2, 113–124, doi:10.5194/amt-2-113-2009, 2009.

Wagner, T., Beirle, S., Dörner, S., Friess, U., Remmers, J., and Shaiganfar, R.: Cloud detection and classification based on MAX-DOAS observations, Atmos. Meas. Tech. Discuss., 6, 10297–10360, doi:10.5194/amtd-6-10297-2013, 2013.